Proceedings of the ASME 2016 35th International Conference on Ocean, Offshore and Arctic Engineering
OMAE2016
June 19-24, 2016, Busan, South Korea

OMAE2016-54813

EXPERIMENTAL STUDY ON FLOW-INDUCED VIBRATION OF FLOATING SQUARED SECTION CYLINDERS WITH LOW ASPECT RATIO, PART II: EFFECTS OF ROUNDED EDGES

Rodolfo T. Gonçalves[1,2]
(rodolfo_tg@tpn.usp.br)

Dennis M. Gambarine[1]
(dennis_maluf@tpn.usp.br)

Aline M. Momenti[1]
(alinemomenti@gmail.com)

Felipe P. Figueiredo[1]
(felipe_pierrobom@tpn.usp.br)

André L. C. Fujarra[3,1]
(andre.fujarra@ufsc.br)

[2] Department of Ocean Technology, Policy, and Environment
School of Frontier Sciences
University of Tokyo
Kashiwa-no-ha, Kashiwa, Chiba, Japan

[1] TPN - Numerical Offshore Tank
Department of Naval Architecture and Ocean Engineering
Escola Politécnica - University of São Paulo
São Paulo, SP, Brazil

[3] Department of Mobility Engineering
Federal University of Santa Catarina
Joinville, SC, Brazil
(Formerly at University of São Paulo)

ABSTRACT

Experiments regarding flow-induced vibration on floating rounded squared section cylinders with low aspect ratio were carried out in an ocean basin equipped with a rotating-arm apparatus. Floating squared section cylinders with rounded edges and aspect ratios of $L/D = 2.0$ were elastically supported by a set of linear springs in order to provide low structural damping to the system. Two different incidence angles were tested, namely 0 and 45 degrees. The Reynolds numbers covered the range from $2,000$ to $30,000$. The aim was to understand the flow-induced vibrations around single columns, gathering information for further understanding the causes for the Vortex-Induced Motions in semi-submersible and TLP platforms. Experiments on circular and squared sections cylinders (without rounded edges) were also carried out to compare the results with the rounded square section cylinders (with rounded edges). The amplitude results for in-line, transverse and yaw amplitude for 0-degree models showed to be higher for squared section cylinders compared to those for the rounded square section cylinders. No significant difference between the 45-degree models was observed. The results of ratio between frequency of motion in the transverse direction and natural frequency in still water confirmed the vortex-induced vibration behavior for the squared and rounded square section cylinders for 45-degree incidence; and also the galloping characteristics for 0-degree incidence cases. The rounded effect on the square section cylinders showed to be

important only for reduced velocity larger than 8, which is probably related to the position of the separation point that changes around the rounded edge, behavior that did not occurr for the squared edge that fixed the separation point for any reduced velocity.

Keywords: flow-induced vibration (FIV), vortex-induced vibration (VIV), vortex-induced motion (VIM), low aspect ratio, floating squared section cylinder, rounded square section cylinder

1. INTRODUCTION

Studies on flow around squared section cylinders can be found for different engineering situations due to their large application. Buildings, bridges and oil and gas platforms are examples of these squared section structures. At the same time, concerns about the interaction between bluff bodies and fluids arise due to the vibration problems observed, leading those structures to an eventual collapse by fatigue. The so-called Flow-Induced Vibrations (FIV) can be separated at least into two different phenomena, called galloping and vortex-induced vibration (VIV), both well known in the engineering segment.

Galloping is a dynamic instability – in one degree of freedom (1dof) – caused by the incidence of fluid flow in a non-circular and slender structure. Classical galloping of non-circular cylinders is caused by a fluid-dynamic instability of the cross section of the body, such that the motion of the structure generates forces which increase the amplitude of vibration, see Bearman *et al*. (1987) [3]. More details about the galloping theory can also be found in Parkinson (1971) [11] and Blevins (1990) [4].

VIV is a typical resonant phenomenon due to vortex shedding around cylinders, according to which cyclic loads can cause an excess of vibration that gives rise to fatigue problems in the structures. Comprehensive reviews about the VIV theory can be found in Bearman (1984) [2] and Blevins (1990) [4].

Initial observations of the interaction between galloping and vortex shedding resonance for rectangular cylinders is presented in Parkinson and Brooks (1961) [10], in which a squared section cylinder was tested with low damping values. Thenceforth, an uncountable number of works were published about experimental studies on this issue, most of them carried out in wind tunnels, varying the geometrical cross section, the damping systems and considering different types of flow. Parkinson and Wawzonek (1981) [12] is an example, the authors described the strong mutual effects of galloping and VIV phenomena. The study was carried out with prisms of different aspect of ratios (height divided by length, 0.375 L/D 2.485) and their results presented two modes of lateral vibration and a torsional mode about the stream wise axis.

Bearman *et al*. (1984) [1] studied squared section cylinders by means of experiments carried out in a water tunnel. A relation between radius and base length (r/D) was used to define the variation in the corners. Two different positions of the flow incidence were tested, 0 degree and 45 degrees, i.e. one with the model faces positioned in a direction of in-line flow and the other with two corners of the cylinder in the in-line flow direction. Force coefficients were measured by strain-gauges, and the results for drag coefficient (C_D) were shown accordingly. For 0-degree incidence, C_D presented a decreasing behavior with an increase of r/D. When the Reynolds number started to increase, the performance of the rounding corner had low values compared with the others. Curiously, difference occurred when the incidence angle was changed to 45 degrees, for cylinders without rounded corners submitted to low Reynolds number, where the drag coefficient results presented higher values ($C_D \cong 5$) compared with the same model in 0-degree incidence ($C_D \cong 3$) . Additionally, by increasing the Reynolds number, the same feature was observed – a decrease of C_D for rectangular cylinders without rounded corners – therefore, the difference between the models were lower compared with the results of 0-degree incidence.

Recently, works in water flow increased due to the offshore demand, e.g. semi-submersible platforms used in large scale for oil and gas exploitation; in some cases, adopting squared section columns linked by submerged pontoons. In fact, the geometry of the semi-submersible platforms implies a complex vortex-induced motion (VIM) phenomenon, as can be found in the works by Waals *et al*. (2007) [15], Rijken & Leverette (2008) [13], Fujarra *et al*. (2012) [5] and Gonçalves *et al*. (2012a, 2013a) [8] [9].

In this context, the present work is the second part of a study on FIV of squared section cylinders. The first part, presented in Gonçalves *et al*. (2015) [7], showed the effects of different aspect of ratios ($L/D = 1.0$, 2.0 and 3.0) placed at 0 and 45 degrees of incidence. The experiments were carried out with floating cylinders – six degrees of freedom (6dof) – and the principal result was the higher amplitudes in the transverse direction for the model positioned at 45 degrees, besides the aspect ratio has not presenting significant variation. The details about results of VIV on circular cylinders with very low aspect ratio are also discussed in Gonalves e Fujarra (2014) [6].

Continuing the investigation on VIV of squared section cylinders, this second part aims to understand the FIV around cylinders with three different cross sections: rounded square section cylinders (herein named RQC); squared section cylinders (herein named SQC) and circular section cylinder for comparisons (herein named CC). All the floating cylinders considering an aspect ratio of $L/D = 2.0$.

Chapter 2 presents the experimental setup of the tests performed. Chapter 3 presents the experimental results comprising non-dimensional amplitudes and frequencies for the transverse direction, in-line direction and yaw motion, presented as a function of the reduced velocity, $V_r = U/(f_{0y}D)$, as well as power spectral density (PSD) for supporting the discussions and con-

clusions. Finally, chapter 4 presents the main conclusions and perspectives for further works.

2. EXPERIMENTAL SETUP

All the experiments were carried out in the Hydrodynamic Calibrator (CH-TPN), which is an offshore basin ($14m \times 14m \times 4m$) located in the Numerical Offshore Tank laboratory at the University of São Paulo (USP), Brazil, equipped with a rotating arm for towing small model and slender bodies.

The rotating arm comprises an arm in stainless steel covered by fiberglass, a vertical pole and two trapezoidal supports mounted on a circular trail centered in the tank. Figure 1 shows dimensions of the main components of this apparatus. For further details, see Vieira *et al*. (2013) [14].

Figure 2 shows our experimental setup for testing the floating cylinders – aluminum bars used to support the springs and instrumentation – attached to the rotating arm. Additionally, Fig. 3 shows an upper view of the experimental setup installed in the rotating arm, $R = 2.84m$.

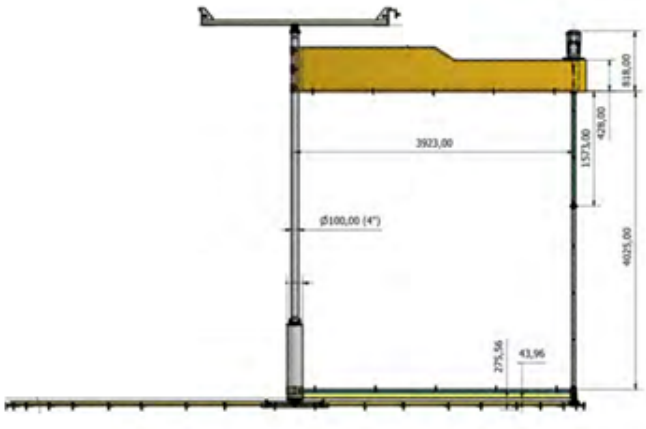

FIGURE 1. **Main dimensions of the rotating arm.**

The angular velocity does not affect the uniform flow. Due to the great size of the arm, $R = 2.84m$, and the small dimension of the characteristic length for each condition tested, $D = 125mm$, the incoming velocity can be considered uniform.

Figure 4 shows the experimental setup where $\dot{\Theta}$ is the angular velocity, k is the springs stiffness. Equations 1 and 2 show the forces acting in the angular movement of the rotating arm for directions X (in-line) and Y (transverse). Due to the low angular velocities,$\dot{\Theta}$, low values of these forces are present, which therefore do not affect the experimental results.

$$m\ddot{x} + 2kx = \bar{F_D} + F_D sin(2\omega_y t + \phi x) - m\dot{\theta}\dot{y} \qquad (1)$$

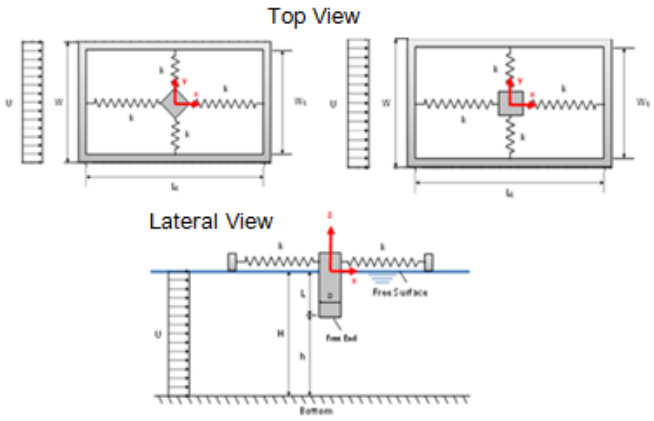

FIGURE 2. **Experimental setup and dimensional parameters for FIV tests.**

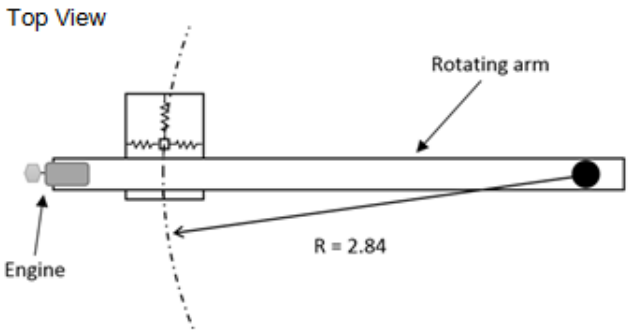

FIGURE 3. **Experimental setup installed in the rotating arm.**

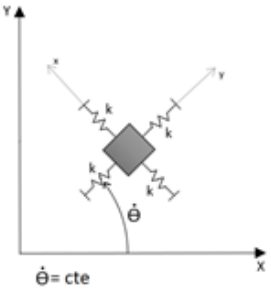

FIGURE 4. **Coordinate of the movements considered.**

$$m\ddot{y} + 2ky = F_L sin(2\omega_y t + \phi y) + m\dot{\theta}^2(R + y) + m\dot{\theta}\dot{x} \qquad (2)$$

Four different cylinders were built, resulting in two SQC cylinders and two RQC cylinders, all with $L/D = 2.00$. The models were made in polyvinyl chloride (PVC); see Fig. 5.

The main parameters of the models are presented in Table 1. Details about the dimension can be seen in Fig. 6 with regards

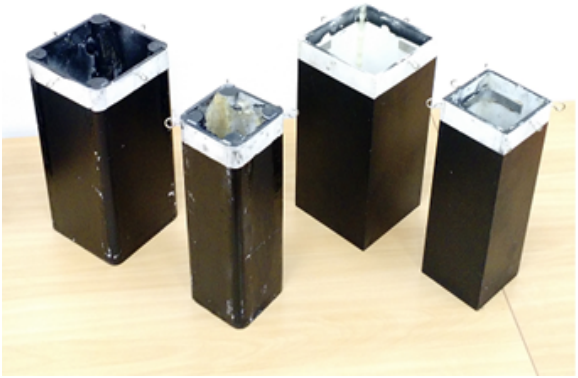

FIGURE 5. **Illustration of PVC models of the cylinders with square sections. On the left side: rounded square cylinders (RQC). On the right side: square section cylinders (SQC). All cylinders with $L/D = 2.00$.**

to the dimensionless parameters L/D and L/A, where L is the length of the squared section. As floating cylinders, all the mass ratios were considered $m^* = 1.00$.

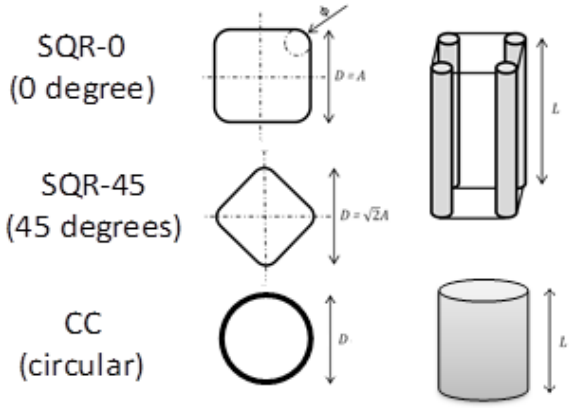

FIGURE 6. **Main parameters of the cylinders tested.**

As mentioned, the floating squared section cylinders were elastically supported by a set of four springs with the same stiffness parameter, $k = 0.8N/m$, in a rectangular support with dimensions of $L_q = 1090mm$ and $W = 610mm$, length and width respectively. The models were free to move in the 6dof, the immersion condition was adjusted changing the ballast inside and the movements were measured by means of an optical motion capture system, QUALISYS ^{TM}. Details in Fig. 7 and 8.

The natural frequencies in still water in both directions were

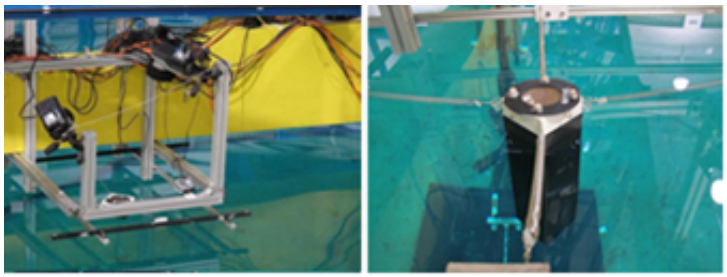

FIGURE 7. **Floating model positioned at 45 degrees, elastically supported by a set of four springs and monitored by an optical motion capture system.**

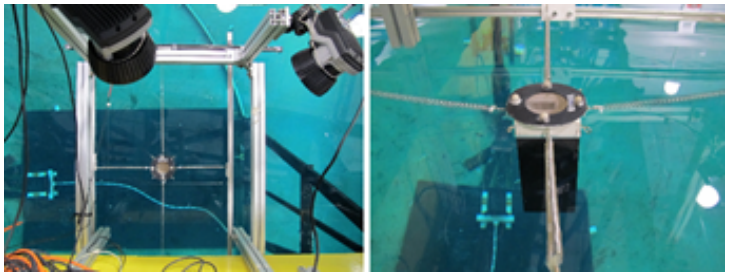

FIGURE 8. **Floating model positioned at 0 degree, elastically supported by a set of four springs and monitored by an optical motion capture system.**

TABLE 1. **Dimensional parameters of the tests.**

ID	Incidence Angle [degree]	D[mm]	A[mm]	L/D	L/A
SQC	0	125.0	125.0	2.0	2.0
	45	125 .0	88.4	2.0	2.8
RQC	0	125.0	125.0	2.0	2.0
	45	125.0	88.4	2.0	2.8
CC	-	125.0	125.0	2.0	-

practically the same for all the models, $f_{0x}/f_{0y} \cong 0.97$ and due to this, it was possible to consider $f_{0x} = f_{0y} = f_0$. The damping coefficient in still water was practically close for all conditions, $\zeta_W \cong 6\%$ (in-line) and $\zeta_W \cong 7\%$ (transverse) and the structural damping very low around $\zeta = 0.1\%$.

About twenty-seven velocity conditions were carried out for each model. The reduced velocity range performed was $2 \leq V_r \leq 15$; therefore, the range of Reynolds number was $2x10^3 \leq Re \leq 3x10^4$, which corresponds to current incidences of $0.02m/s \leq$

$U \leq 0.23m/s$. Details about the conditions tested are presented in Table 2.

The effect of the wake of the previous run can be neglected, as the time spent for each test condition is sufficiently large to attenuate it. As the tests were conducted for velocities up to $0.2m/s$; no wave making of models were observed. The accuracy and stability of the towing speed is very high due to the active control of the rotating arm.

As mentioned, the 6dof were measured throughout the tests. A form factor $\gamma = 1.0$ was used to determine the non-dimensional characteristic amplitudes. In both directions the non-dimensional characteristic amplitudes were calculated as the mean of the 10% largest peaks and the characteristic frequency as the peak frequency in the power spectral density (PSD) of the motion history.

Only the results for in-line, transverse direction and yaw motions are presented. The results for other degrees of freedom were small and did not influence the FIV behavior, which is the reason for the authors not to include those results in this paper.

TABLE 2. Parameters of the tests for each aspect ratio condition.

ID	Angle [degree]	$Rex10^4$	ζ_W [%]	f_{0x} [Hz]	f_{0y} [Hz]	f_{0yaw} [Hz]
SQC	0	$0.25 \rightarrow 1.92$	7.54	12.61	12.18	2.77
	45	$0.35 \rightarrow 2.66$	7.89	12.48	12.31	2.45
RQC	0	$0.34 \rightarrow 2.59$	6.71	9.27	9.06	1.62
	45	$0.37 \rightarrow 2.80$	5.21	9.07	8.81	1.48
CC	-	$0.33 \rightarrow 2.50$	4.64	8.96	8.39	1.67

3. EXPERIMENTAL RESULTS

Figures 9, 10 and 11, respectively show the results for transverse, in-line and yaw motion amplitudes for the case of squared section cylinders (SQC), rounded squared section cylinders (RQC) and circular section cylinder (CC), all with $L/D = 2$. The non-dimensional amplitudes in the transverse direction, $A_y/(\gamma D)$, for SQC-45 and RQC-45 (45-degrees incidence) presented significant higher values for $V_r > 4$, compared with the SQC-0 and RQC-0 cases (0-degree incidence), see Figure 9. These results confirm that the rounded edges changed the onset of the increase in amplitudes for the SQC. Moreover, SQC-0 showed a steady growth when the reduced velocity was increased, which is similar to a galloping feature. Note that RQC-0 presented a similar growth, as described previously, yet with amplitudes lower than SQC-0 for $V_r > 8$. Therefore, the rounded edge effects greatly decrease the amplitudes for this case at higher values of reduced velocity. SQC and RQC cases presented smaller amplitudes compared to the CC ones for $V_r > 6.5$.

Figure 10 shows the non-dimensional amplitudes in the in-line direction, $A_x/(\gamma D)$. Comparable values were found for squared cylinders (with or without rounded edges) at $Vr \leq 6$. Henceforth, CC presented different and higher growth, a typical VIV feature. In turn, the SQC-0 presented higher amplitudes for high reduced velocities, $V_r > 13$. Moreover, no significant differences were found between RQC-0 and RQC-45.

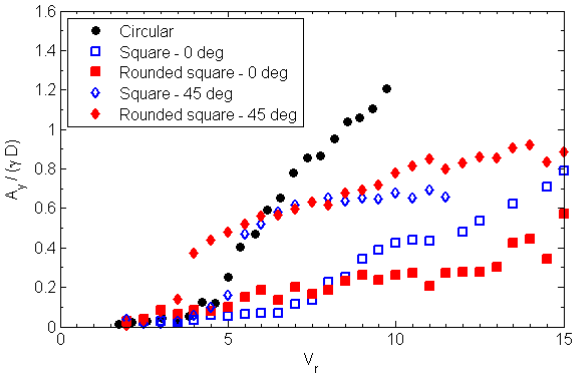

FIGURE 9. Non-dimensional motion amplitude in the transverse direction ($A_y/(\gamma D)$) as a function of reduced velocity (V_r) for cylinders with different sections (SQC - squared section and RQC - rounded squared section) with $L/D = 2.0$.

The high yaw amplitudes were a very important feature for observing the galloping phenomenon. Based on this, it was possible Figure 11 allows observing higher values of yaw amplitude for the SQC and RQC cases compared with the CC ones, mainly for higher values of reduced velocity. Also for the yaw motions, RQC-0 performed notable lower values at $V_r > 13$ compared to those for SQC-0.

The result of the ratio between the transverse motion frequency and the natural transverse frequency in still water (f_y/f_0) is presented in Figure 12. For RQC-0 and SQC-0, the frequency ratio presented a constant behavior in the range of reduced velocity $V_r \leq 8$, possibly because it was not possible to observe a VIV phenomenon for these cases. Differences were observed for 45-degree models for higher reduced velocities, SQC-45 presented a linear increase, whereas RQC-45 presented constant values, $f_y/f_0 \cong 1$.

Results of the ratio between the in-line and transverse frequency (f_x/f_y) are shown in the Figure 13. Frequency ratios

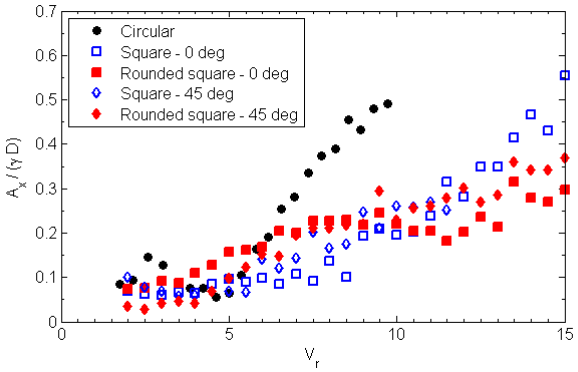

FIGURE 10. **Nondimensional motion amplitude in the in-line direction ($A_x/(\gamma D)$) as a function of reduced velocity (V_r) for cylinders with different sections (SQC - squared section and RQC - rounded squared section) with $L/D = 2.0$.**

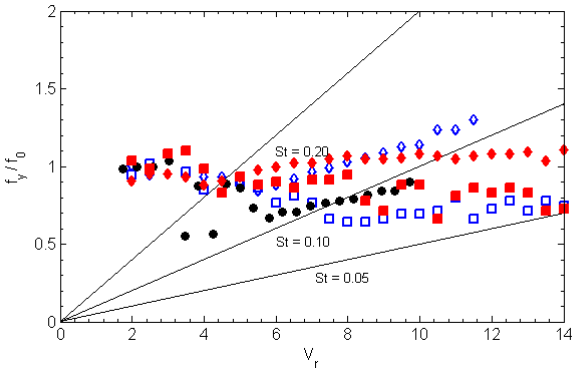

FIGURE 12. **Ratio between the transverse motion frequency and the natural transverse frequency in still water (f_y/f_0) as a function of reduced velocity (V_r) for cylinders with different sections (SQC - squared section and RQC - rounded squared section) with $L/D = 2.0$.**

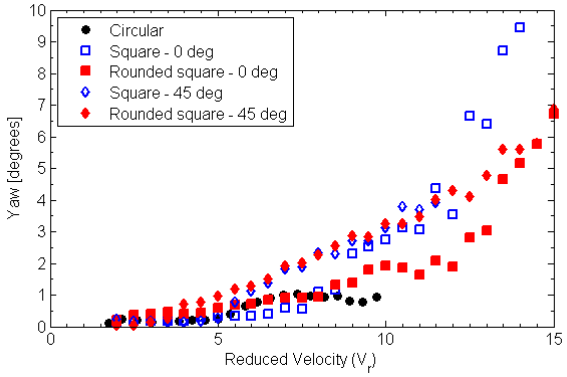

FIGURE 11. **Yaw motion amplitude (A_{yaw}) as a function of reduced velocity (V_r) for cylinders with different sections (SQC - squared section and RQC - rounded squared section) with $L/D = 2.0$.**

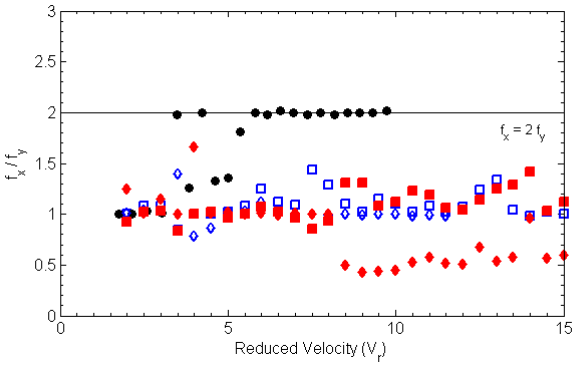

FIGURE 13. **Ratio between in-line and transverse motion frequencies (f_x/f_y) as a function of reduced velocity (V_r) for cylinders with different sections (SQC - squared section and RQC - rounded squared section) with $L/D = 2.0$.**

for SQC and RQC showed the in-line frequency motion similar to the transverse one, $f_x \cong f_y$, exception observed for RQC-45, where the transverse motion showed twice larger frequencies than in-line ones, $f_y \cong 2f_x$ – this behavior was clearly different in terms of the trajectories of movement. On the other hand, circular cylinders (CC) presented an opposite behavior; the frequency ratio showed values equal to two, $f_x/f_y \cong 2$, corresponding to a usual VIV characteristic of 8-shaped trajectories of movement.

Figure 14 presents the results of the ratio between yaw frequency and natural transverse frequency in still water (f_{yaw}/f_0). CC and SQC-45 performed similar behavior as was observed for ratio f_y/f_0, i.e. linear growth when reduced velocity was increased. In addition, a constant trend can be observed for RQC-0.

Results of PSD for the in-line, transverse and yaw motions are presented in Figure 15 to 19 as a function of the reduced velocity, confirming the statements up to this point.

For RQC-0, the energy of in-line, transverse and yaw motions showed to be concentrated around the natural frequency of the system in still water, and this energy increased with the increase of the reduced velocity; see the behavior in Figure 15. For SQC-0, the same behavior can be observed; however, the yaw showed higher energy, see Figure 17. This larger energy was possibly due to the excessive yaw movement, thus representing a galloping characteristic.

Comparing 45-degree cases, the rounded edges seem not affect the system energy for all the movements analyzed. The energy concentrated around natural frequency in still water and in-

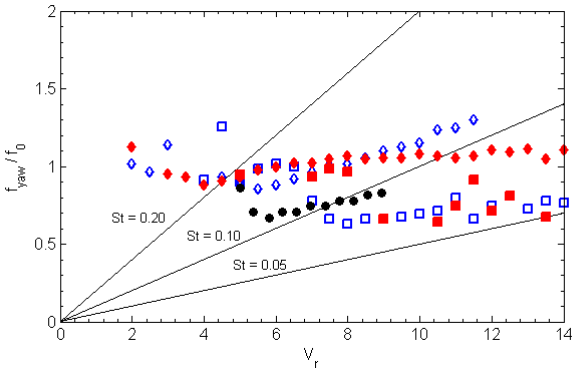

FIGURE 14. **Ratio between the yaw motion frequency and the natural transverse frequency in still water (f_{yaw}/f_0) as a function of reduced velocity (V_r) for cylinders with different sections (SQC - squared section and RQC - rounded squared section) with $L/D = 2.0$.**

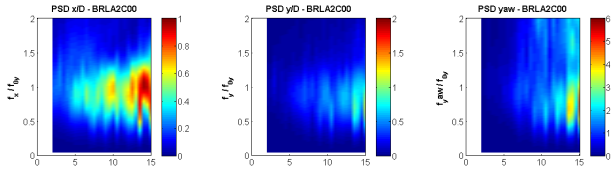

FIGURE 15. **PSD of the motion in the in-line direction, transverse direction and yaw as a function of V_r for RQC - rounded squared section cylinder with $L/D = 2.0$ and 0-degree incidence.**

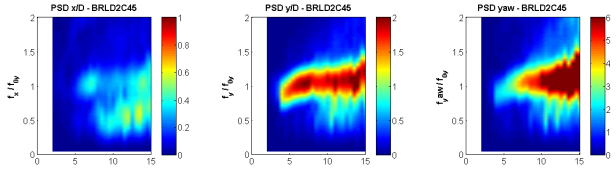

FIGURE 16. **PSD of the motion in the in-line direction, transverse direction and yaw as a function of V_r for RQC - rounded squared section cylinder with $L/D = 2.0$ and 45-degree incidence.**

creased when reduced velocity was increased. Figure 16 and 18 show details.

CC presented in-line energy concentrated near frequency ratio equal to two, and low energy for yaw motion. However, CC, SQC-45 and RQC-45 cases presented similar results for energy level in the transverse direction, i.e high energy concentrated around the natural frequency in still water. Therefore, these results show a typical VIV feature, details in Figure 19, 16, 18.

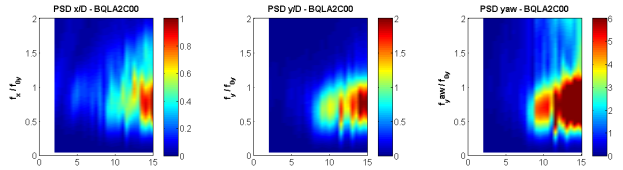

FIGURE 17. **PSD of the motion in the in-line direction, transverse direction and yaw as a function of V_r for SQC - squared section cylinder with $L/D = 2.0$ and 0-degree incidence.**

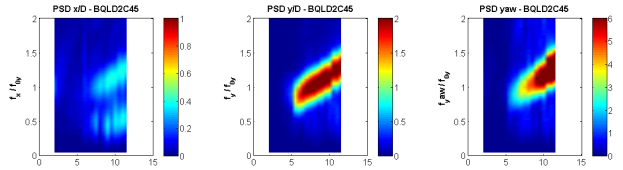

FIGURE 18. **PSD of the motion in the in-line direction, transverse direction and yaw as a function of V_r for SQC - squared section cylinder with $L/D = 2$ and 45-degree incidence.**

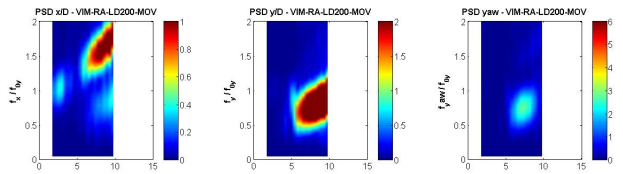

FIGURE 19. **PSD of the motion in the in-line direction, transverse direction and yaw as a function of V_r for CC - circular section cylinder with $L/D = 2.0$**

4. GENERAL CONCLUSIONS

The present work was motivated by the VIM studies around single columns of multicolumn platforms, aiming to understand the effects of the rounded edges in squared section cylinders under two different angles of incidence. For comparisons, results of a circular cylinder was also considered.

The experiments were carried out in an ocean basin equipped with a rotating arm apparatus at TPN. Three different shapes were tested, namely squared section cylinder (SQC), rounded squared section cylinder (RQC) and circular section cylinder (CC), at 0 and 45 degrees of incidence angle. The models were free to oscillate (6dof), presenting the same aspect ratio, $L/D = 2.0$.

Non-dimensional amplitudes were presented for in-line, transverse and yaw motions. Rounded squared cylinder with 0-degrees incidence (RQC-0), presented lower values for the transverse direction, compared to cylinder without rounded edge with the same angle (SQC-0). The circular cylinder (CC) exhibited the higher values for transverse and in-line amplitudes; however, the rounded edge did not cause effects for in-line amplitudes; re-

sults in Berman (1984) [1], with high velocities, presented similar results. Yaw amplitudes showed higher for square section models due to the influence of the galloping phenomenon in these bodies, in addition to the observation of significant higher values for SQC-0 compared to RQC-0.

Analysis of the frequency ratio showed important results for the models placed in 45 degrees. A similar behavior can be observed for ratios of transverse and yaw motion by natural frequency in still water, f_y/f_0 and f_{yaw}/f_0 respectively, which means a linear growth for the square cylinder (SQC-45) and a constant value for the rounded edge model (RQC-45) under an increase of reduced velocity.

Finally, results for PSD were analyzed for the models. Despite the 0-degree incidence angle of the square section cylinders, important difference occurred for yaw movement energy, showing higher values for the non-radius model (SQC-0); a typical galloping phenomenon behavior. On the other hand, the behavior of SQC and RQC were similar for models with 45-degrees incidence. Moreover, the transverse amplitudes for these cases can be compared with CC case, knowing a typical behavior of the VIV phenomenon, as stated by Zhao *et al*. (2014) [16].

The rounded effect on the square section cylinders showed to be important only for reduced velocity $V_r \geq 8$, i.e. the position of the separation point of the boundary layer changed around the rounded edge, behavior that can not occurr for the squared edge that fixed the separation point for any reduced velocity. The amplitudes showed to be higher for RQC-45 than SQC-45, which can be explained by the VIV behavior for this incidence angle, i.e. the rounded edge contributed to large synchronization between the frequency of the motions and the frequency of vortex shedding. On the other hand, the amplitudes showed to be lower for RQC-0 than SQC-0, which can be explained by the galloping behavior for this incidence angle, i.e. the rounded edge contributed to modifying the lift forces variation that characterized the galloping behavior.

This work is a continuity of Gonçalves *et. al.*(2015) [7], in which the authors showed a complete analysis of the influence of aspect of ratio with different angles of incidence applied to squared section cylinders.

NOMENCLATURE

γ Modal form factor
ϕ Phase angle
ω_y Angular oscillation frequency in the transverse direction
ζ_s Structural damping
ζ_W Damping coefficient in still water
$A_x/(\gamma D)$ Characteristic non-dimensional motion amplitude in the in-line direction
$A_y/(\gamma D)$ Characteristic non-dimensional motion amplitude in the transverse direction
D Characteristic diameter
f_0 Natural frequency in still water, both in in-line and transverse directions
f_{0x} natural frequency of the system in still water at the in-line direction
f_{0y} natural frequency of the system in still water at the transverse direction
f_{0yaw} yaw motion natural frequency of the system in still water
f_s Vortex-shedding frequency
f_x Oscillation frequency in the in-line direction
f_y Oscillation frequency in the transverse direction
f_{yaw} Oscillation frequency in the transverse direction
F_D Drag force
F_L Lift force
H Water height of the tank
k Spring Stiffness
L Immersed length
L_q Rectangular apparatus length
m System mass
m^* Mass ratio
m_d Displaced mass
m_s Structural mass
L/D Aspect ratio
Re Reynolds number
U Flow velocity
x Displacement in the in-line direction
$\dot{x}$ Velocity in the in-line direction
$\ddot{x}$ Acceleration in the in-line direction
y Displacement in the transverse direction
$\dot{y}$ Velocity in the transverse direction
$\ddot{y}$ Acceleration in the in-line transverse direction

ACKNOWLEDGMENT

The authors would like to acknowledge Petrobras and the National Petroleum and Natural Gas Agency (ANP) for the financial support. Prof. Dr. Andr Fujarra acknowledges CNPq (National Council for Scientific and Technological Development, Brazil) for the financial support, grant 309591/2013-9". Dr. Rodolfo Gonçalves acknowledges the São Paulo Research Foundation (FAPESP), process number 2014/02043-1, and the University of Tokyo for the financial support.

REFERENCES

[1] BEARMAN P.W., GRAHAM, J.M.R., & OBASAJU E.D., DROSSOPOULOS G.M. The influence of corner radius on the forces experienced by cylindrical bluff bodies in oscillatory flow. *Appl Ocean Res* 6:8389, 1984.

[2] BEARMAN P.W. Vortex Shedding from Oscillating Bluff Bodies. *Annual Review of Fluid Mechanics* Vol. 16:

195-222, 1984.

[3] BEARMAN P.W., GARTSHORE. S. , MAULL D. J., & PARKINSON, G. V. . Experiments on Flow-Induced Vibration of a Square-section Cylinder. *Journal of Fluids and Structures* 19-34, 1987.

[4] BLEVINS, R.D. Flow-Induced Vibration. *2nd edn. Van Nostrand Reinhold.*

[5] FUJARRA, A. L. C., ROSETTI, G. F., WILDE, J. & GONÇALVES, R. T. State-of-art on vortex-induced motion: A comprehensive survey after more than one decade of experimental investigation. *Proceedings of the 31st International Conference on Ocean, Offshore and Arctic engineering.* Rio de Janeiro, Brazil - OMAE2012-83561, 2012.

[6] GONÇALVES, R.T., FUJARRA. Experimental study on vortex-induced vibration of floating circular cylinders with low aspect ratio. *Proceedings of the 33st International Conference on Ocean, Offshore and Arctic engineering.* San Francisco, California, USA - OMAE2014-23383, 2014.

[7] GONÇALVES, R.T., GAMBARINE, D.M., FIGUEIREDO, F.P., AMORIM F.V., &FUJARRA, A. L. C. Experimental study on flow-induced vibration of floating squared section cylinders with low aspect ratio, Part I: Effects of incidence angle. *Proceedings of the 34th International Conference on Ocean, Offshore and Arctic engineering.* St. Johns, NL, Canada - OMAE2015-41008, 2015

[8] GONÇALVES, R.T., ROSETTI, G.F., FUJARRA, A.L.C. & OLIVEIRA, A.C. Experimental study on vortex-induced motions of a semi-submersible platform with four square columns, Part I: Effects of current incidence angle and hull appendages. *Ocean engineering.* Vol. 54, pp. 150-169, 2012a.

[9] GONÇALVES, R.T., ROSETTI, G.F., FUJARRA, A.L.C. & OLIVEIRA, A. C. Experimental study on vortex-induced motions of a semi-submersible platform with four square columns, Part II: Effects of surface waves, external damping and draft condition. *Ocean engineering.* Vol. 62, pp. 10-24, 2013a.

[10] PARKINSON, G.V., & BROOKS, N.P.H. On the aeroelastic instability of bluff cylinders. *Journal applied mechanics* 28 (2), 252258, 1961

[11] PARKINSON, G.V. Wind-induced instability of structures. *Philosophical Transactions for the Royal Society of London. Series A* Vol 269, issue 1199, 1971

[12] PARKINSON, G.V, & Wa. Some considerations of combined effects of galloping and vortex resonance. *Journal of Wind Engineering and Industrial Aerodynamics.* 8(1-2), 135143, 1981

[13] RIJKEN O. & LEVERETTE S. Experimental study into vortex induced motion response of semi-submersible with square columns. *Proceedings of 27th international Conference on Offshore Mechanics and Arctic Engineering.* Estoril, Portugal - OMAE2008-57396, 2008.

[14] VIEIRA, D.P., MALTA, E.B., GONÇALVES, R.T. & FUJARRA, A.L.C. Development of a rotating arm system to study VIV phenomena in an offshore basin. *Proceedings of the 22nd International Congress of Mechanical Engineering (COBEM 2013).* Ribeiro Preto, SP, Brazil, 2013.

[15] WAALS, O.J., PHADKE, A.C., & BULTEMA, S. Flow induced motions of multi column floaters. *Proceedings of the 26th International Conference on Offshore Mechanics and Arctic Engineering.* San Diego, California, USA - OMAE2007-29539, 2007.

[16] ZHAO, M. & CHENG, L. Vortex-induced vibration of a circular cylinder of finite length. *Physics of Fluid.* Vol. 26, pp. 015111, 2014.